

# Comparisons of Ground Motions from Colocated and Closely Spaced One-Sample-per-Second Global Positioning System and Accelerograph Recordings of the 2003 M 6.5 San Simeon, California, Earthquake in the Parkfield Region

by Guo-Quan Wang,\* David M. Boore, Guoqing Tang, and Xiyuan Zhou

**Abstract** The 2003 San Simeon, California, earthquake (M 6.5) generated a set of colocated and closely spaced high-rate (1-sample-per-second) Global Positioning System (GPS) positions and ground motions from digital accelerographs in the Parkfield region (at epicentral distances of 50 to 70 km). The waveforms of displacements derived from the 13 GPS receivers in the region have dominant periods between about 7 and 18 sec. The waveforms are similar in shape, with a systematic change in waveform as a function of distance from the source. The GPS motions are smaller than the accelerograph motions for periods less than about 2 sec. From this we conclude that the 1-sample-per-sec GPS receivers provide a good representation of ground motion at periods longer than about 2 sec. Perhaps more important for earthquake engineering is that the accelerograph data are similar to the GPS data for periods as long as 30 sec, if not longer. This means that data from digital accelerographs can provide reliable relative-displacement response spectra at the periods needed in the design of large structures, at least for earthquakes with magnitudes of 6.5 or above at distances within 70 km. We combine the colocated or very closely spaced GPS and accelerograph data sets in the frequency domain to obtain a single broadband time series of the ground motion at each accelerograph station. These broadband ground motions may be useful to seismologists in unraveling the dynamic process of fault rupture and to engineers for designing large structures with very-long-period response.

## Introduction

GPS has traditionally been used to measure long-term, annual-to-decade, tectonic deformation and static displacements from large earthquakes. In the past few years, 1-sample-per-sec continuously sampled GPS data have been used to measure strong earthquake ground motions at periods longer than about 5 sec (e.g., Larson *et al.*, 2003; Bock *et al.*, 2004; Irwan *et al.*, 2004), and these motions have been used in inversions for the fault slip for several earthquakes (e.g., Ji *et al.*, 2004; Miyazaki *et al.*, 2004). The 1-sample-per-sec GPS motions, often referred to as “high-rate GPS motions,” may also be useful in earthquake engineering. Until recently, engineering design was concerned mainly with periods less than 5 sec, and the ground motions for design have been obtained from accelerographs. Very large struc-

tures, however, have resonant periods at or beyond the upper limit of most analog-recording accelerographs (about 5 sec), and in addition, much emphasis is currently being placed on displacement-based design, which requires ground motions at periods longer than normally considered in the past (e.g., Bommer and Elnashai, 1999; Faccioli *et al.*, 2004). Digital accelerographs have the potential to provide reliable ground motions at longer periods (e.g., Boore, 2005a), but often have difficulties in recovering long-period motions (e.g., Iwan *et al.*, 1985; Boore, 2001, 2003; Wang *et al.*, 2003; Boore and Bommer, 2005). There is an overlap in the ranges of periods for which the 1-sample-per-sec GPS and the accelerograph data provide reliable measures of ground motions, and thus it is natural to combine the two types of data recorded at a particular site in a single direction into a single broadband record of ground motion. This combined motion will significantly increase the observable frequency band for earthquake ground motions from any one type of recording and will be

\*Present address: Department of Geology, University of Puerto Rico, P.O. Box 9017, Mayaguez, Puerto Rico 00681-9017; gwang@uprm.edu.

useful in traditional seismological studies of seismic-wave propagation and dynamic fault rupture process, as well as for engineering seismology and earthquake engineering.

Some previous studies have found good agreement between 1-sample-per-sec GPS positions and long-period motions from nearby accelerographs for several earthquakes: 2002 Denali ( $M$  7.9) (Larson *et al.*, 2003; Bock *et al.*, 2004), 2003 Tokachi-Oki, Japan ( $M$  8.0) (Clinton, 2004; Irwan *et al.*, 2004; Miyazaki *et al.*, 2004; Emore *et al.*, 2007), and 2003 San Simeon ( $M$  6.5) (Ji *et al.*, 2004). One common feature of these comparisons is that they are limited mainly to visual comparisons of displacement waveforms in the time domain. In this study, we use comparisons in the frequency domain, as quantified by 5%-damped relative-displacement response spectra (in essence, the displacement of a suite of damped single-degree-of-freedom oscillators with natural periods ranging from a small fraction of a sec-

ond to tens or hundreds of seconds). In this article we analyze ground motions of the 22 December 2003 San Simeon, California, earthquake ( $M$  6.5) recorded on 13 1-sample-per-sec GPS receivers in the Parkfield region (at epicentral distances ranging from 33 km to 71 km, with most being near 65 km) and five accelerographs sited near the GPS stations (see Fig. 1 and Table 1). Almost the same set of GPS and accelerograph stations recorded the  $M$  6.0 2004 Parkfield earthquake, which was much closer to the stations than was the San Simeon earthquake. We study the San Simeon earthquake instead of the Parkfield earthquake in this article for several reasons, the primary one being that we want to compare the similarity in waveforms of the GPS displacements over the set of stations as a means of checking the reliability of data; this is more easily done using a set of stations whose interstation spacing is much less than the distance from the source, as we would expect smaller changes in waveforms

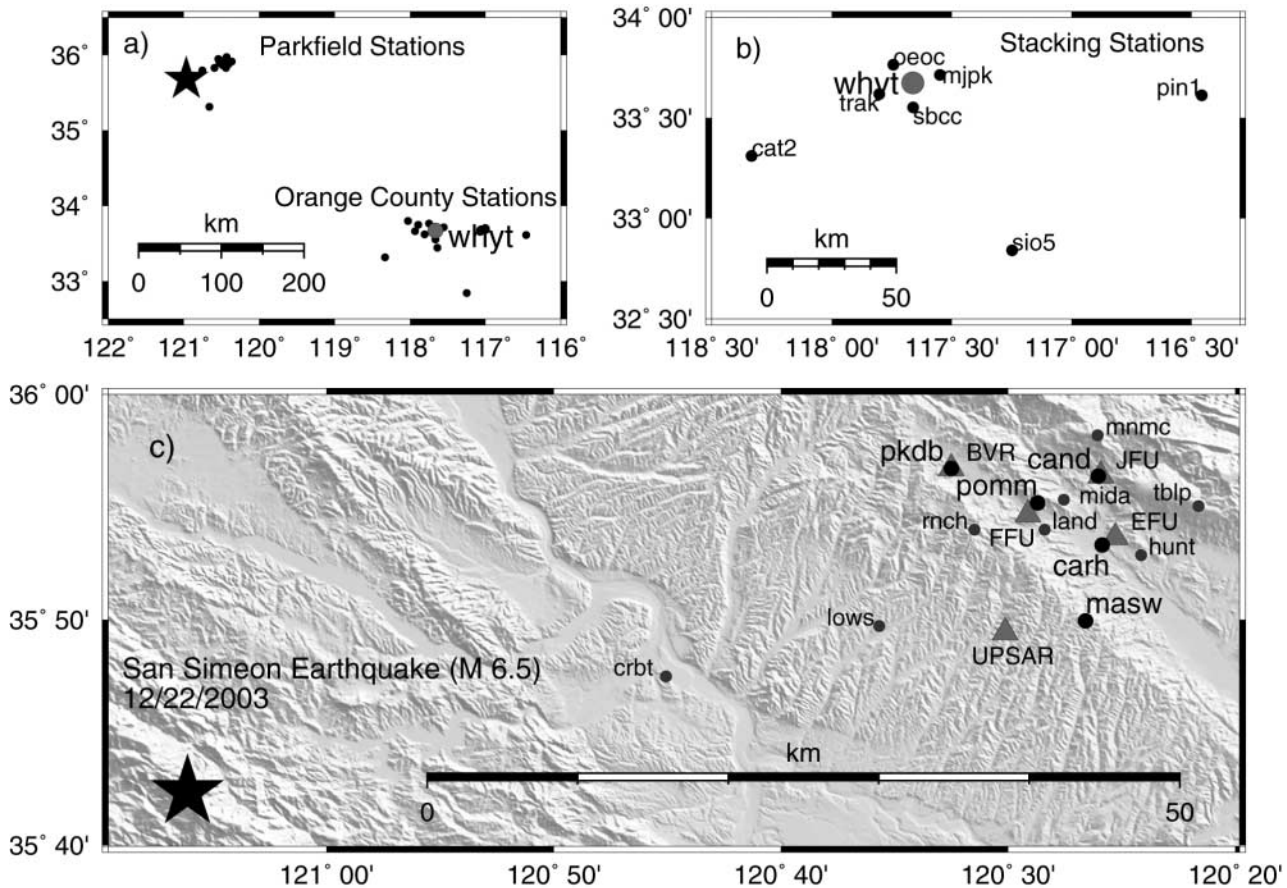


Figure 1. Maps showing locations of the 2003 San Simeon earthquake, 1-sample-per-sec GPS stations, and strong ground-motion accelerograph stations studied in this article. (a) 1-sample-per-sec GPS stations in the Parkfield region and in Orange County. We set whyt as the reference GPS station in this study. (b) Specific locations of the seven stacking stations which belong to the Orange County Real Time Network. (c) A shaded relief map showing the epicenter of the 2003 San Simeon earthquake, locations of accelerograph stations BVR, FFU, JFU, EFU, and UPSAR (gray triangles), and locations of thirteen GPS stations (black circles). The location of the epicenter ( $-121.102, 35.706$ ) is from the website of the California Integrated Seismic Network (CISN, <http://www.quake.ca.gov/cisn-edc/idr/2003.htm>)

Table 1  
Locations of Colocated and Closely Spaced GPS and ACC Instruments Studied in This Article

Station Name	Instrument Type*	Latitude	Longitude	Sample Rate (sps) <sup>†</sup>	Sta.-to-Sta. Distance (km) <sup>‡</sup>
BVR	FBA	35.9452	-120.5415	80	0
pkdb	GPS	35.9452	-120.5415	1	
FFU	FBA	35.9111	-120.4855	200	1.0
pomm	GPS	35.9199	-120.4784	1	
JFU	FBA	35.9397	-120.4319	200	0.2
cand	GPS	35.9393	-120.4336	1	
EFU	FBA	35.8942	-120.4212	200	1.0
carh	GPS	35.8883	-120.4308	1	
UPSAR	FBA	35.8240	-120.5021	200	5.3
masw	GPS	35.8326	-120.4430	1	

\*FBA, force balance accelerometer; GPS, Global Positioning System receiver.

<sup>†</sup>sps, samples per sec.

<sup>‡</sup>The numbers are the distances between consecutive pairs of stations in the table, e.g., 5.3 is the distance in kilometers between UPSAR and masw.

than if the stations were near the source (spatial similarity of waveforms has proven to be a useful way of checking the reliability of the long-period content of accelerograph data—e.g., Hanks, 1975; Boore *et al.*, 2002). In addition, we wanted to limit the scope and length of this article (we note that preliminary comparisons of the GPS and accelerograph recordings for the Parkfield earthquake agree with the results in this article).

Following this introduction, the article begins with a brief description of the GPS and accelerograph data and data processing. We then show that the GPS waveforms are similar spatially, indicating that they provide reliable measures of long-period ground motions and that the GPS data can be used to test the validity of the accelerograph data at longer periods. Comparing the GPS and accelerograph data, we find that the GPS data become deficient in energy relative to the accelerograph data for periods less than about 2 sec. More importantly, we also find that the ground motions for the accelerograph data are very similar to the GPS motions for periods greater than about 4 sec and extending to periods as long as 30 sec, if not longer. Finally, in view of the limitations of the GPS data at short periods and the accelerograph data at long periods, we exploit the advantages of each data set by combining them into a single broadband record of ground displacement at each accelerograph site.

## Data and Data Processing

### One-Sample-per-Sec GPS Data and Data Processing

One-sample-per-sec ground-motion displacements from thirteen GPS receivers in the Parkfield region are available from the 22 December 2003 San Simeon earthquake. The stations, indicated by lower-case station codes, are shown in Figure 1; they are part of the Southern California Integrated GPS Network (<http://www.scign.org>). Langbein and Bock (2004) reported that these continuously recording 1-sample-per-sec receivers near Parkfield can be used to estimate horizontal displacements of order 0.6 cm at the 99% confidence

level from a few seconds to a few hours, and Ji *et al.* (2004) report standard deviations of 0.3, 0.7, and 1.1 cm for the east–west, north–south, and vertical displacements, respectively. In a controlled laboratory setting, Elósegui *et al.* (2006) find errors generally less than 0.5 cm from shake table tests.

The 1-sample-per-sec GPS raw data, which is in binary MBEN format, is converted into Rinex format using program “teqc” (<http://www.unavco.ucar.edu/software/teqc>), and then processed in the following three steps as illustrated in Figure 2. GPS positions at the time 19:15:00, UTC, 22 December 2003 are adjusted to zero in this study.

*Step 1: Initial Processing.* We first process the GPS data with GAMIT-GLOBK software packages using the kinematic data-processing program TRACK (Chen, 1998). Station whyt is set as a reference station in our data processing, which is about 350 km away from the earthquake source (see Fig. 1a). We use this station as a reference because the coseismic displacements should be very small. One-sample-per-sec GPS positions on day 355 (21 December 2003, one day before this earthquake) and day 356 (22 December 2003) are extracted from the raw data (Fig. 2a). No filtering is applied in this processing.

*Step 2: Sidereal Filtering.* We then perform sidereal filtering (Fig. 2b) on the GPS positions (day 356) based on the positions on day 355 to reduce multipath and other diurnally repeating noises. The idea of sidereal filtering is generally attributed to Genrich and Bock (1992). It is a technique that has been used to improve high-rate GPS positions to take advantage of the ground-track repeat period of satellites. We use the modified sidereal filtering introduced by Choi *et al.* (2004). The sidereal period is set as 23h55m55s (245 sec less than one day). It is an average of the orbit repeat times for all visible satellites during the period of the earthquake shaking. Estimated positions on day 355 are high-cut (low-pass) filtered with a 7-sec running mean to reduce high-

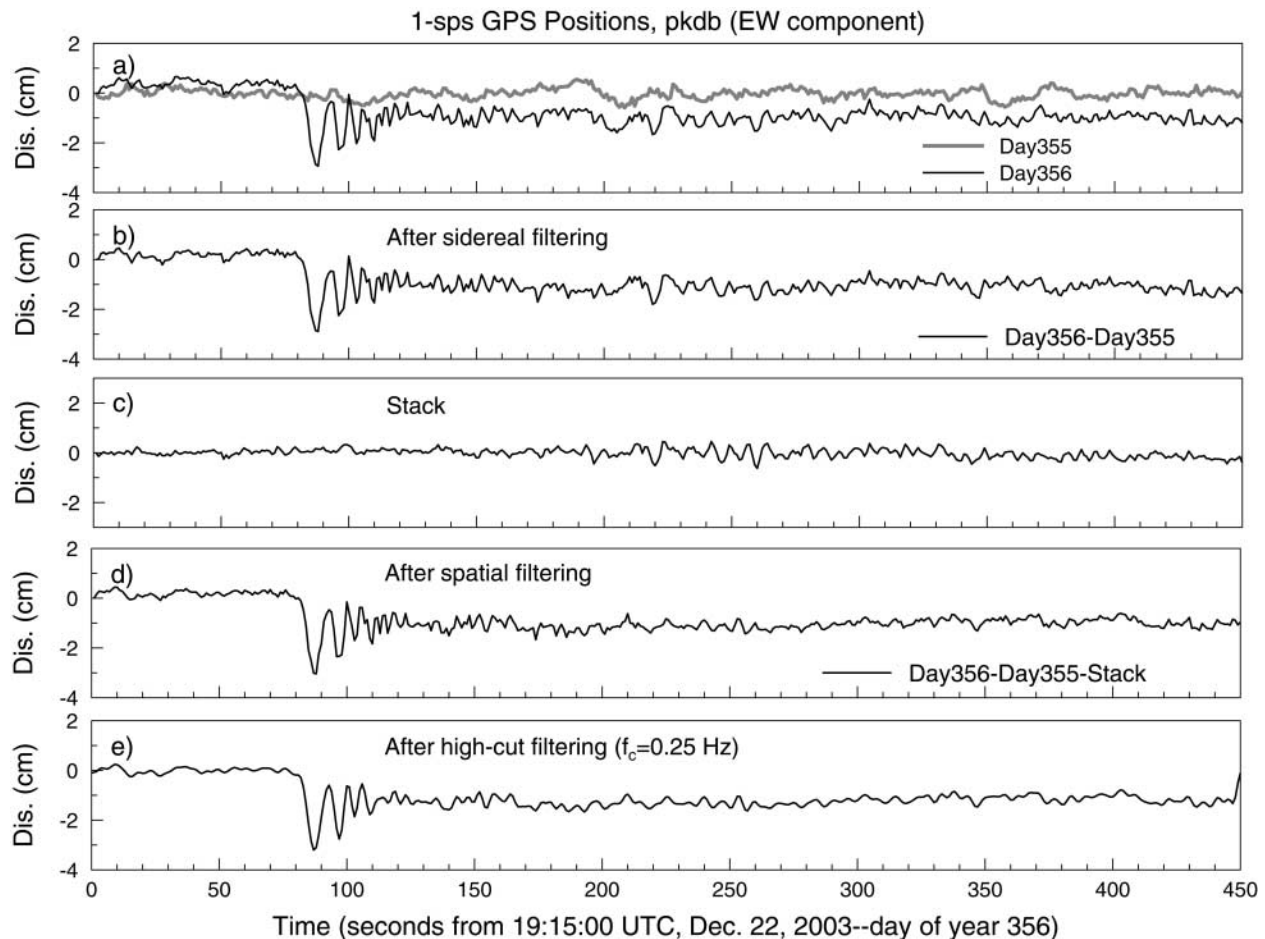


Figure 2. Plots showing data processing of 1-sample-per-sec GPS data. (a) GPS positions extracted from raw data using program TRACK of GAMIT-GLOBK. The positions of day 355 are shifted backward one day minus 245 sec. (b) GPS positions after sidereal filtering (day 356 minus day 355). (c) Stack of seven stationing illustrated in Figure 1b. (d) GPS positions after subtracting the stack (b - c). (e) GPS positions after applying a high-cut (low-pass) filter at 0.25 Hz.

frequency noise before being reduced from the estimated positions on day 356.

**Step 3: Spatial Filtering–Stacking.** Next we perform spatial filtering (Fig. 2d) using a stacking (Fig. 2c) of seven sites (cat2, sio5, pin1, trak, sbcc, mipk, and oeoc) from the Orange County Real Time Network. Stacking is a technique introduced by Wdowinski *et al.* (1997) to remove “common-mode” errors. The locations of these stacking stations are plotted in Figure 1a, b.

**Step 4: High-Cut (Low-Pass) Filtering.** A high-cut (low-pass) Butterworth acausal filter is applied to the sidereal-spatial-filtered 1-sample-per-sec GPS displacements (Fig. 2e) to remove high-frequency noise. The corner frequency of the high-cut filtering is set at 0.25 Hz, for reasons discussed later. This filtering, as well as the low-cut filtering used in processing the accelerograph data, is achieved by two passes of a time-domain causal fourth-order Butterworth filter, with

the second pass through the time series produced by the first pass, but reversed in time. The result is a filter response that goes as  $f^8$  and  $1/f^8$  for the low-cut and high-cut filters, respectively.

To compute relative-displacement response spectra (SD) and to combine the GPS data with the accelerograph data, we interpolate (upsample) the GPS data to the sample rate of the corresponding accelerograph data (80 samples per sec for BVR, 200 samples per sec for the other stations) and then convert the displacements to accelerations using a five-point central second-difference operator. We prefer to do the upsampling using the fast Fourier transform (FFT) procedure discussed by Brigham (1988, p. 199), in which the transform beyond the Nyquist frequency is extended with zeros. This procedure guarantees that frequency components higher than the Nyquist frequency are not introduced into the interpolated time series. We found, however, that when we doubly integrated the resulting acceleration time series back to displacements, long-period trends were introduced

that were difficult to remove with simple baseline corrections. Although it is possible to find a series of small corrections to the baseline of each acceleration time series, constrained such that the displacement will approximately match the original GPS displacement (adapting the procedures used by Nikolaidis *et al.*, 2001, and Emore *et al.*, 2007), we found that upsampling using a cubic-spline interpolator required only the addition of a very small pulse at the beginning of the record to have agreement with the original displacement. For this reason, this interpolator was used for all results shown in this article, although a small amount of high-frequency energy might be introduced into the record. Extensive numerical experimentation shows that the difference resulting from the various interpolators is not important for the results of this article. The low-cut (high-pass) filtering referred to later, as well as the computation of SD, was performed on the GPS data converted to accelerations. Displacements were derived by double integration of the filtered acceleration time series.

#### Accelerograph Data and Data Processing

In this article we study all pairs of GPS and digital accelerograph stations in the Parkfield region that are located within a bit more than 5 km of one another—there were five such pairs (Fig. 1, Table 1). One of the accelerograph stations is collocated with the GPS station pkdb. This station, located at the Bear Valley Ranch, was given the station code PKD by the operating agency (the University of California Berkeley Seismographic Station), but we refer to it as BVR to avoid confusion with the collocated GPS station (we use capital letters for the accelerograph station codes to distinguish them from the lower-case GPS station codes). Three of the other accelerograph stations (FFU, JFU, EFU) are three U.S. Geological Survey (USGS) General Earthquake Observation System (GEOS) stations (Borcherdt *et al.*, 1985; [http://nsmg.wr.usgs.gov/data\\_sets/20031222\\_1915.html](http://nsmg.wr.usgs.gov/data_sets/20031222_1915.html)); the final accelerograph station (UPSAR) is taken from USGS Parkfield Dense Seismograph Array (UPSAR) (Fletcher *et al.*, 1992), which covers an area smaller than 0.5 km<sup>2</sup> and consists of 14 irregularly spaced seismograph stations (P01–P14). Wang *et al.* (2006) found that the middle and long-period motions (e.g., >3 sec) are very consistent among these stations. The acceleration data from P06 was arbitrarily selected to represent the motions at UPSAR in this study. The epicentral distances of these stations are about 65 km (see Fig. 1). The distance between the pairs of stations is given in Table 1; the largest interstation spacing that we consider in this article is 5.3 km (for masw and UPSAR).

As deployed in the Parkfield region, the GEOS (FFU, JFU, and EFU) accelerograph includes a 1-pole, 0.1-Hz low-cut (high-pass) hardware filter (G. Glassmoyer, personal comm., May 2005). The response of this filter falls off slowly enough, and the signal strength is large enough, that we could deconvolve the traces. We did this by dividing the instrument-filtered accelerations by the impulse responses of the instru-

ment filters in the frequency domain. We also apply a low-cut (high-pass) filter at 0.02 Hz to counteract the amplification, produced by the deconvolution operator, of the long-period noise. As an example, we illustrate the relative-displacement response spectrum for both the original instrument-filtered and the deconvolved accelerations from FFU-EW in Figure 3.

Ji *et al.* (2004) show that it is possible to recover the finite offset of the ground following the earthquake (the residual displacement) for the BVR station. In our experience, however, the apparent residual displacements can be very sensitive to the processing parameters, and for this reason we have chosen not to attempt a recovery of the residual displacements. Instead, we show results in which low-cut (high-pass) filters are applied to accelerograph data in which the only processing is the removal of a mean, either determined from the pre-event portion if available, or from the whole record. The filtering, discussed previously, included zero pads to account for the filter transients, as discussed in Boore (2005b). To avoid truncation effects, the data preceding the first zero-crossing and following the last zero-crossing are replaced with zeros as suggested by Converse and Brady (1992). Response spectra are computed from the padded, filtered accelerations, and velocity and displacement time series are obtained by integration of the padded, filtered acceleration time series.

#### Spatial Comparison of GPS Ground Motions

A good way of evaluating, in a qualitative way, the accuracy of ground-motions obtained from seismographic instruments is to compare visually the waveforms of motions

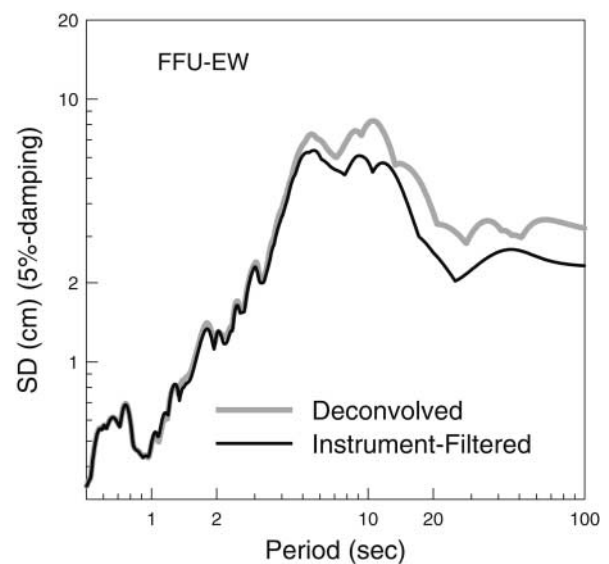


Figure 3. An example of 5%-damped relative-displacement response spectra (SD) calculated from the deconvolved GEOS accelerograph data. Black trace represents the original, instrument-filtered data (FFU-EW); gray trace represents deconvolved data.

at periods long enough that variations in local site response should not strongly affect the motions (e.g., Hanks, 1975). We do that in Figure 4, which shows the three-component displacements at five of the thirteen GPS stations. The gray lines are displacements after applying a high-cut (low-pass) filter at 0.25 Hz (this hardly affects the comparisons shown in the figure, as the GPS displacements have little energy at frequencies higher than about 0.25 Hz), and the black lines show the displacements after applying an additional low-cut (high-pass) filter at 0.01 Hz. In agreement with Ji *et al.* (2004), the figure shows that the high-cut-only displacements for the north–south and up–down components are more uncertain than for the east–west component. Applying a low-cut (high-pass) filter, however, removes much of the noise, and the dominant portions of the waveforms are seen to be quite similar to one another. In the rest of this article we concentrate on the east–west component of motion.

When plotted as a “record section” in order of increasing distance from the source (Fig. 5), the waveforms of the displacements from the GPS receivers are similar in shape, with a clear change of the waveforms with distance. The displacement traces are dominated by two groups of energy, with the time separation between the groups increasing with distance. These two groups are simply the *P* and *S* waves

from the source, as can be inferred by plotting the times of the troughs of each group against distance to the hypocenter and distance to the point of maximum slip on the fault (according to the slip model of Ji *et al.*, 2004). A regression line fit to the arrival times for either measure of distance yields velocities close to 5.0 and 2.6 km/sec, respectively (Fig. 6a). These are typical velocities for *P* and *S* waves in the shallow crust. The first energy group, which we identify as the *P* waves, appears to longer period than the second group, which is opposite the usual pattern for *P* and *S* waves. It could be that directivity has compressed the *S*-wave energy to some extent.

The peak amplitudes show an overall decrease with distance, with scatter typical of ground-motion observations (Fig. 6b). The station with the lowest value of displacement is pkdb. As will be shown shortly, the displacements from the colocated accelerograph station BVR are almost identical with those from pkdb, which tell us that the low amplitudes are real and not a result of an instrumental problem or an affect of the GPS data processing. In Figure 7 we compare the relative-displacement response spectra (SD) for all of the GPS stations. In that figure we use different line types for a few of the stations whose SD is sufficiently different from the mass of values to be identified, crbt and lows are closer

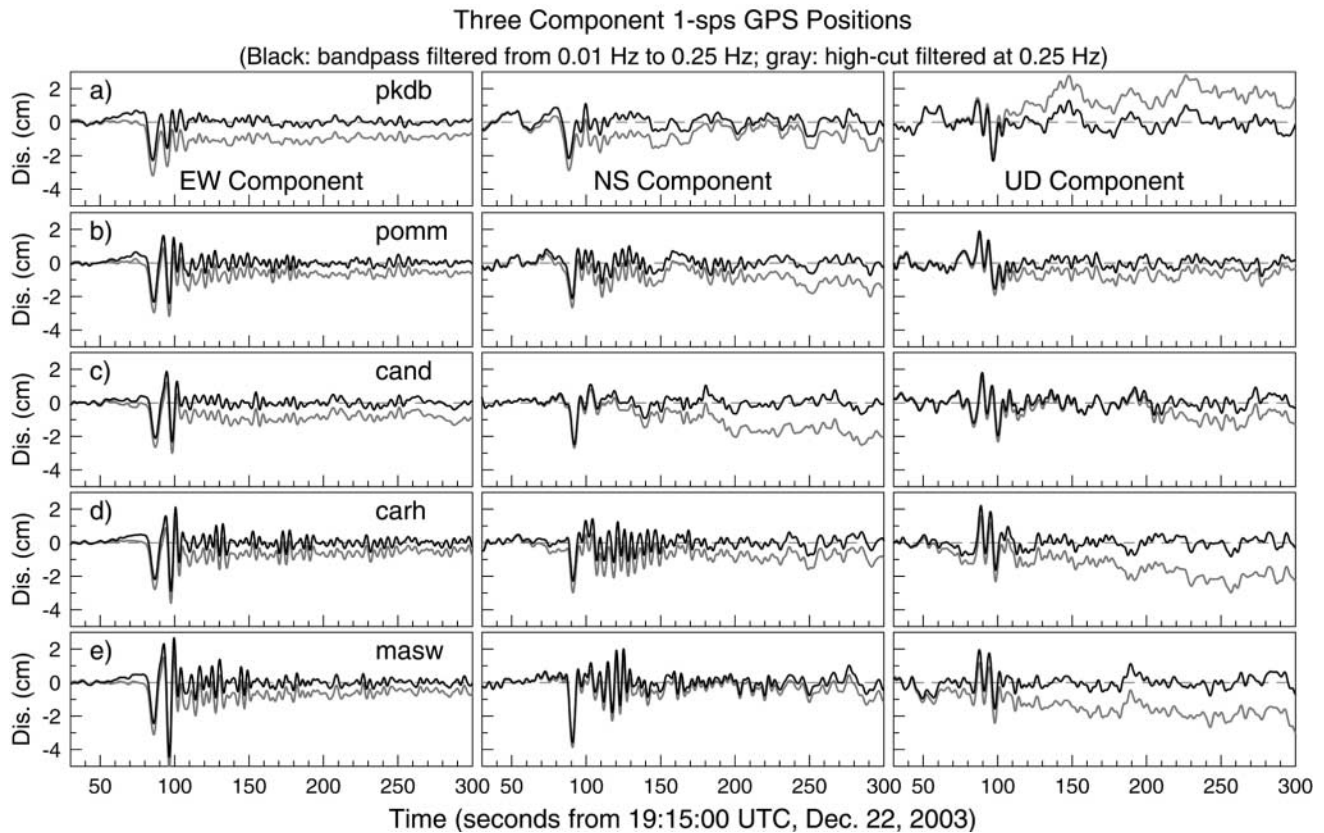


Figure 4. Three-component 1-sample-per-sec GPS positions at stations pkdb, pomm, cand, carh, and masw. Gray traces represent GPS positions processed according to the steps illustrated in Figure 2. Black traces represent GPS positions after applying an acausal low-cut (high-pass) filter ( $f_c = 0.01$  Hz) to the gray traces.

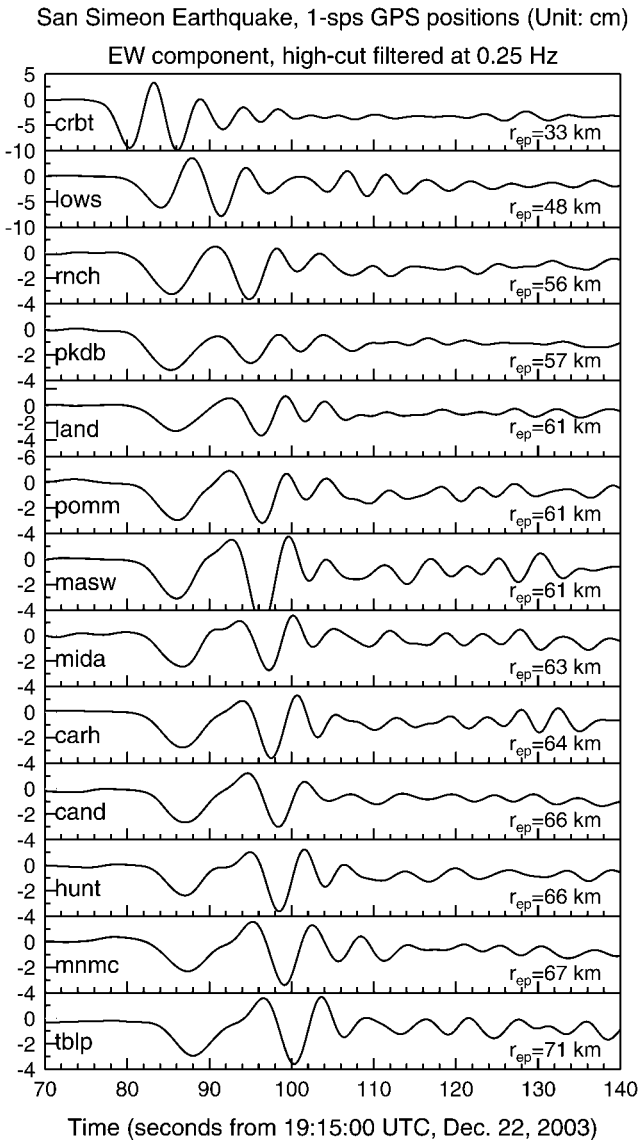


Figure 5. One-sample-per-sec GPS positions (east–west component) at thirteen GPS receivers from the 2003 San Simeon earthquake, after applying an acausal high-cut (low-pass) filter ( $f_c = 0.25$  Hz).

to the source than the other stations, and therefore have larger amplitudes, as would be expected. On the other hand, pkdb and masw are almost at the same distance, and yet their amplitudes are smaller and larger than all other SD from stations in the Parkfield region. The difference exists over most of the period range, implying a very broadband site effect (directivity would affect all of the stations in the region almost equally). (Note that at long periods the SD for pkdb is comparable to that from several other stations. Because a property of SD is that the long-period asymptote approaches the peak displacement in the record, this seems inconsistent with Fig. 6. But as shown in Fig. 5, the true peak displacement for pkdb occurs in the first group of energy, not the second group, whose amplitude is plotted in

Fig. 6.)

The consistency of the waveforms for the GPS displacements gives us confidence that they provide a reliable measure of ground motions at the periods dominating the waveforms. Those motions will be taken as the “truth,” at least at periods larger than the Nyquist period of 2 sec, against which motions derived from the accelerograph recordings will be checked.

### Comparisons with Ground Motions from Accelerometers

As shown in Figure 8, the relative-displacement response spectra from the GPS receivers become much smaller than those from the accelerographs for periods less than about 2 sec. This is not surprising, because the sampling rate of 1-sample-per-sec implies that the GPS motions should have no energy below the Nyquist period of 2 sec (we have been unable to discern whether the GPS receivers use an antialiasing filter or time averages that have the effect of reducing the shorter-period energy in the records). So that this difference in motion at short periods has minimal impact on the comparisons at longer periods, which are of most interest to us, we filtered both the GPS and the accelerograph motions with a 0.25-Hz high-cut (low-pass) filter. We chose a filter of 0.25 Hz (4 sec) as a compromise between removing too much long-period energy from the GPS displacements and including too much short-period motion from the accelerograph-derived displacements (as the bottom two traces in Fig. 2 show, the filtering had little effect on the GPS displacements). An additional advantage to the filtering is that it will reduce site-to-site variability for sites that are not collocated (we expect more variability in site response at short periods than at long periods).

The high-cut (low-pass) filtered ground displacements for the two GPS–accelerograph station pairs with the smallest and the largest interstation spacings are compared in Figure 9 (pkdb–BVR, 0 km spacing, and masw–UPSAR, 5.3 km spacing). The top panel compares the displacements without any low-cut (high-pass) filtering. As is commonly found with digital accelerograph data, large drifts are seen in the displacements derived from the accelerographs. The rest of the panels show the results of removing the long-period motions in both the GPS and the accelerograph-derived displacements, with the filter-cutoff frequency varying systematically from low to high frequency (0.005 Hz to 0.1 Hz). This comparison indicates that accelerograph data provide reliable ground motions to periods of at least 30 sec or longer (at the collocated pkdb–BVR pair, the comparison is good for a filter period of 100 sec). Figure 10 illustrates the same comparison of the relative-displacement response spectra (SD). The SDs of pkdb and BVR agree with one another to periods as long as 100 sec, whereas the SDs of masw and UPSAR agree with each other from 10 to 25 sec, though the two stations are separated by 5.3 km. Figure 10 also illustrates the point that the SD from recordings on digital ac-

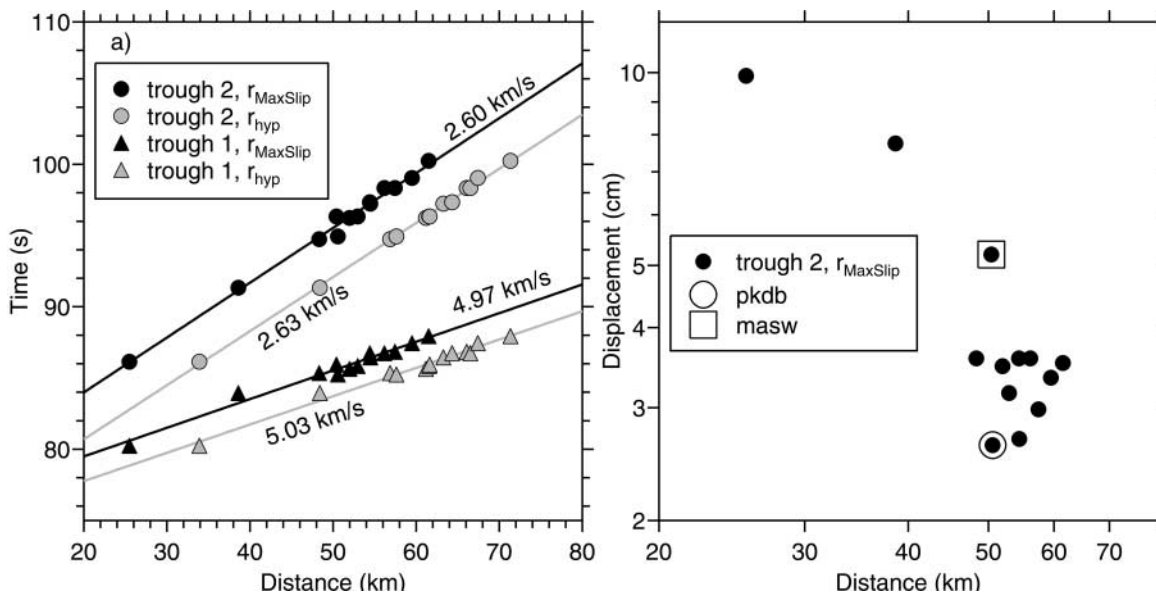


Figure 6. (a) Arrival time of the first and second obvious troughs in the displacement waveforms shown in Figure 5, plotted versus distance to the hypocenter and distance to the center of maximum slip in Ji *et al.*'s (2004) model. The point of maximum slip is 17.6 km southeast of the epicenter (at a bearing of 121° clockwise from north). Also shown are regression fits to the data; the velocity near each line is the inverse of the slope of the line. (b) The maximum absolute displacement of the two troughs, plotted versus distance to maximum slip; stations pkdb and masw are indicated by the circle and square, respectively.

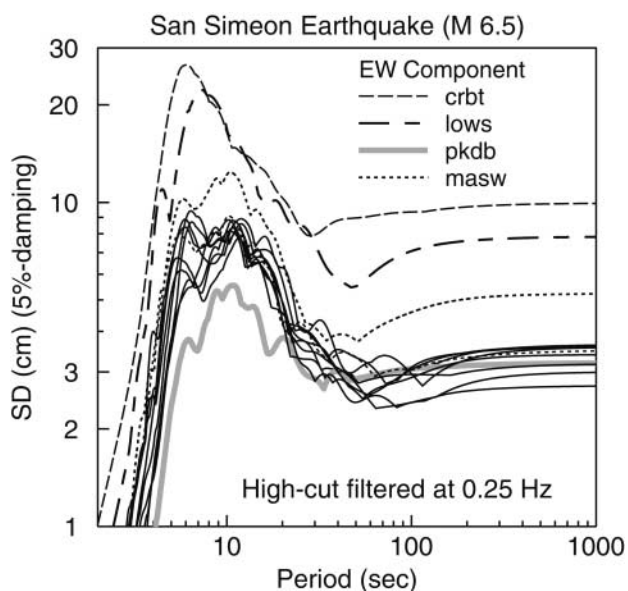


Figure 7. 5%-damped relative-displacement response spectra (SD) calculated from the 1-sample-per-sec GPS data shown in Figure 5. Only selected stations have been distinguished by line type, for reasons explained in the text.

celerographs at periods of most engineering concern (in general, less than 20 sec) is often insensitive to the long-period noise usually contained in the data.

The comparison of SD for the other station pairs is shown in Figure 11 (that figure also shows the pkdb–BVR comparison, but at an expanded period scale compared with Fig. 10). In this case a 0.04-Hz low-cut (high-pass) filter was applied to the motions before computing SD. The SDs are in good agreement over most the period range.

The displacements for the four most closely separated station pairs are shown in Figure 12, but now all three components are shown. The filtering was the same as in the previous figure. As indicated by the title of the abscissa, all traces are plotted relative to the same origin time. The agreement between the GPS and the accelerograph-derived displacements is excellent, except for the vertical component of the pomm–FFU pair. Note that the vertical displacements from all the GPS displacements in the figure have similar waveforms, which suggests that the mismatch for the pomm–FFU pair is due to inaccuracy in the accelerograph-derived displacements for this particular station and component.

#### Combining the GPS and Accelerometer Data: Broadband Ground-Motion Data

The comparisons in the previous section demonstrate that the GPS and accelerograph recordings are complementary: the GPS instruments give the best representation of

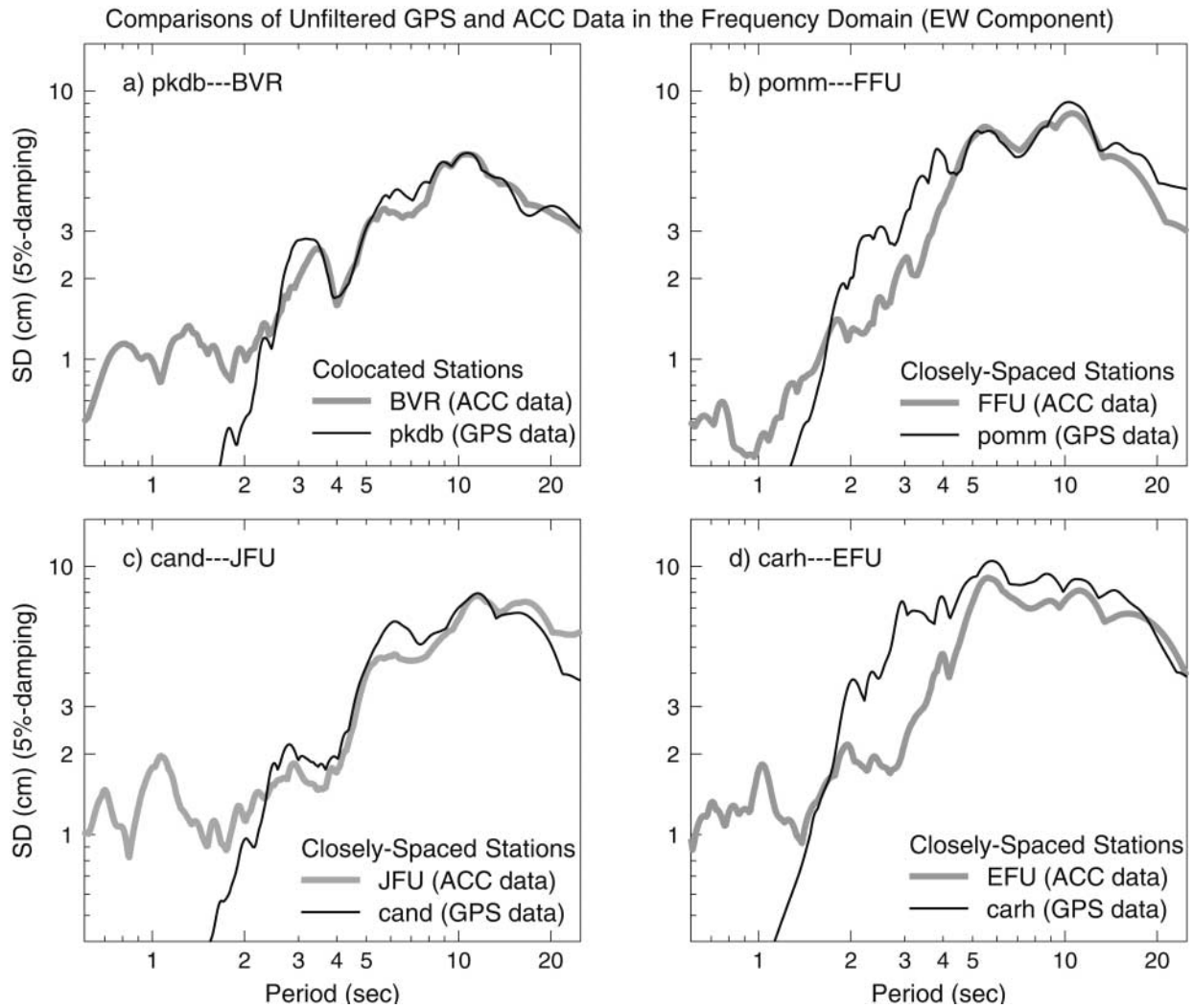


Figure 8. 5%-damped relative-displacement response spectra (SD) calculated from unfiltered accelerograph (ACC) and GPS data.

ground motions at low frequencies and the accelerographs are best at high frequencies. Fortunately, the ground motions from both data sets are similar in the overlapping range between 5 sec to at least 15 sec. We exploit this agreement to combine the two estimates of ground motion into a single-broadband time series for each component of motion at each accelerograph station. (We state that the broadband motion is for the accelerograph station and not the GPS station because we expect station-to-station differences to be larger at high frequencies than at low frequencies, such that the GPS ground displacements are probably a good representation of the ground motion at a nearby accelerograph station. But the converse is not true—the ground accelerations at the accelerograph station are probably not a good representation of the ground accelerations at the GPS stations, because the correlation of ground acceleration decreases rapidly with increasing station separation as shown, e.g., in Appendix A of Boore *et al.*, 2003). We used the procedure introduced by Harvey and Choy (1982) to combine the data. We work with

the acceleration time series, obtained as indicated in the data-processing section. We take the Fourier transforms of each type of data, filter each with a transition filter, add the filtered transforms, and transform back to the time domain. The transition filter applied to the GPS data can be any filter whose response decreases monotonically from unity at the transition frequency  $f_1$  to zero at transition frequency  $f_2$ . The filter applied to the accelerograph data is simply one minus the GPS transition filter. We use a raised cosine filter response, as given in the following equation for the filter applied to the GPS data; Harvey and Choy (1982) used a linear ramp between  $f_1$  and  $f_2$ .

$$f_{hc} = \begin{cases} 1 & f < f_1 \\ 0.5 \times [1 + \cos(\pi(f - f_1)/(f_2 - f_1))] & f_1 < f < f_2 \\ 0 & f > f_2 \end{cases} \quad (1)$$

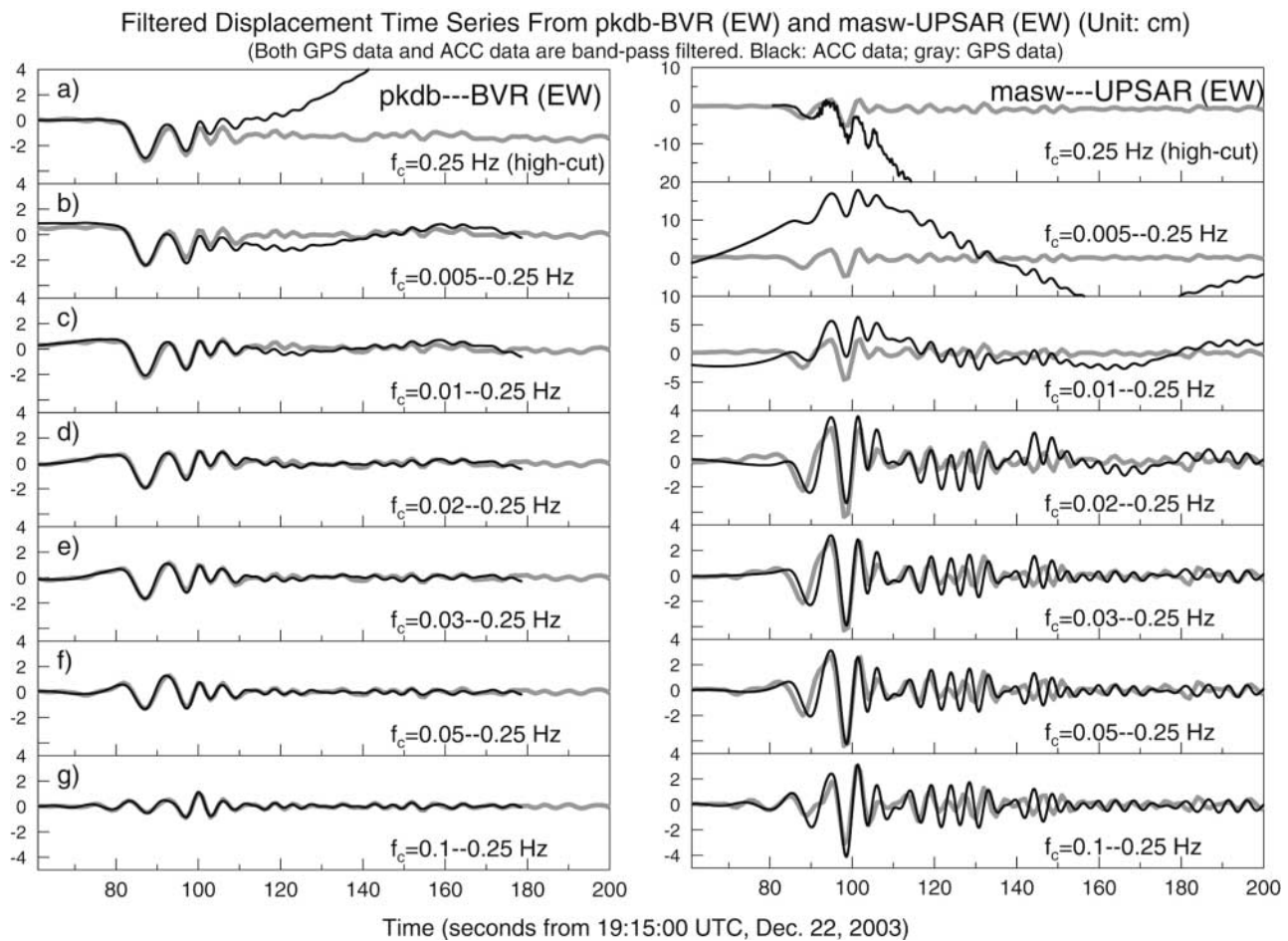


Figure 9. Comparisons of GPS and accelerograph (ACC) data filtered with different low-cut (high-pass) corner frequencies (see text for information about the filters). The left column is for the colocated GPS and ACC pair (pkdb-BVR, east-west). The right column is for the 5.3-km-spaced GPS and ACC pair (masw-UPSAR, east-west). Gray traces represent 1-sample-per-sec GPS data; black traces represent ACC data (80 samples per sec for BVR, 200 samples per sec for UPSAR-P06). Corner frequencies are marked in each subfigure.

and for the low-cut filter applied to the accelerograph data,  $f_{lc} = 1 - f_{hc}$ . The merged data are  $F_{gps} \times f_{hc} + F_{acc} \times f_{lc}$  in the frequency domain, where  $F_{gps}$  and  $F_{acc}$  are the complex Fourier transforms of the GPS and the accelerograph data, respectively.

We illustrate in Figure 13 the process in the frequency domain for the east-west component at the colocated pkdb-BVR station pair. The transition band is set from 0.07 Hz ( $f_1$ ) to 0.2 Hz ( $f_2$ ) based on the previous comparisons. An inverse Fourier transform gives the broadband acceleration shown in the lower left-hand part of Figure 14. That figure also shows the ground motions derived solely from the GPS and the accelerograph data (for the GPS data, the velocities and accelerations were obtained by applying a difference operator to the upsampled displacements; for the accelerograph data, the velocities and displacements were obtained by integration of the accelerations, as were the velocities and displacements of the combined broadband ground motions). The advantages of the broadband data are clearly seen in Figure

14, as the accelerations do not have the small amplitudes of those from the GPS data and the displacements are not plagued by the large drift seen in the accelerograph data. We show the broadband accelerations, velocities, and displacements for the four accelerograph stations most closely located to the GPS stations in Figure 15, with the GPS motions also shown for comparison. In all cases, the broadband accelerations are greater than the GPS-derived accelerations, and the broadband displacements are similar to the GPS displacements, as expected. The relative-displacement response spectra for these broadband time series are given in Figure 16. These spectra might be useful in determining the spectra to be used in displacement-based design of engineered structures.

### Summary

We studied ground motions obtained from 13 1-sample-per-sec (“high-rate”) GPS stations in the Parkfield region that recorded the 2003 San Simeon, California, earthquake

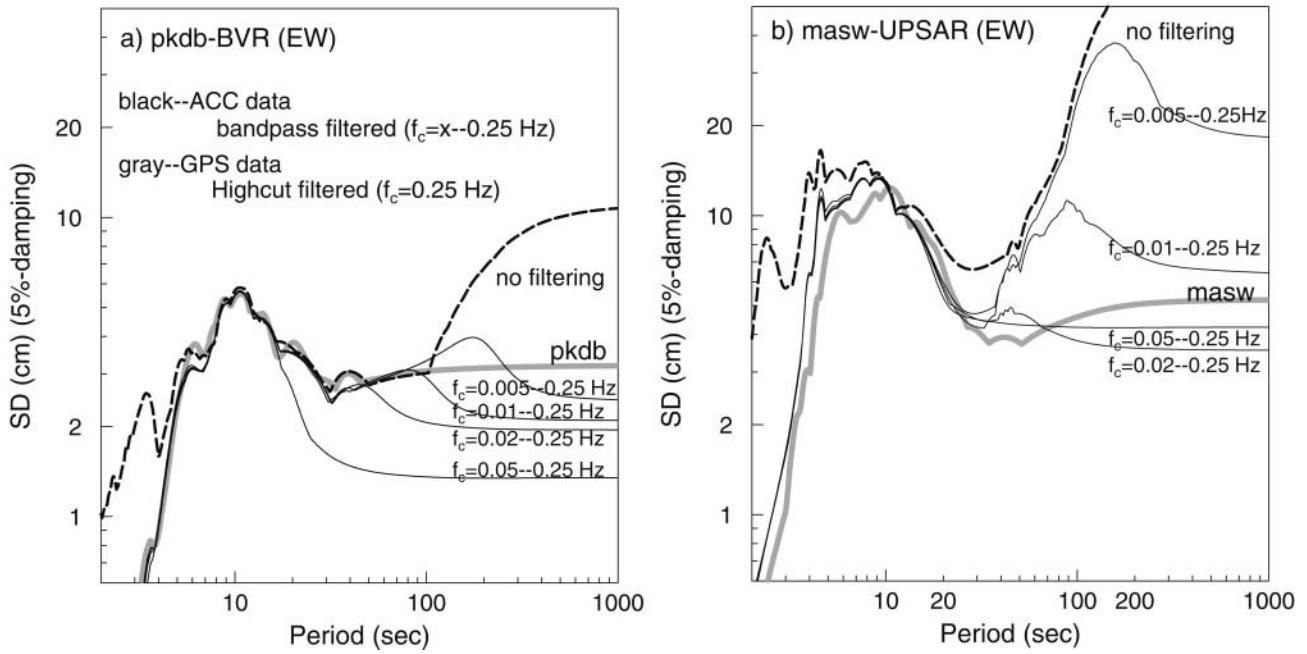


Figure 10. Comparison of 5%-damped response spectral displacement (SD) for 1-sample-per-sec unfiltered GPS data and unfiltered and filtered accelerograph (ACC) data. The station pairs with the smallest and largest station spacing are used in this figure (pkdb-BVR, 0 km, and masw-UPSAR, 5.3 km, respectively).

Comparisons of Bandpass Filtered (0.04--0.25 Hz) GPS and ACC Data in the Frequency Domain

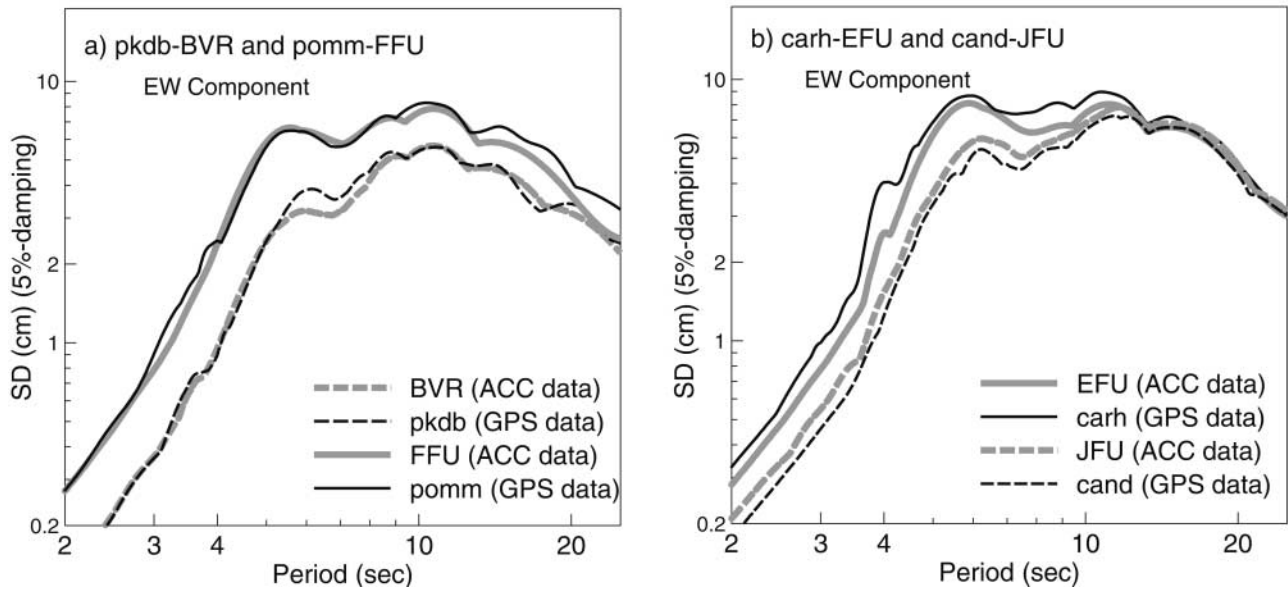


Figure 11. 5%-damped relative-displacement response spectra (SD) calculated from bandpass-filtered accelerograph (ACC) and GPS data.

(M 6.5). We found that the ground displacements from these recordings had consistent waveforms, with two obvious wave arrivals with propagation velocities of 5.0 and 2.6 km/sec (presumably *P* and *S* waves from the source). The consistency of the waveforms indicated to us that the displacements from the GPS instruments are good measures of the

true ground displacements. We used these displacements (and the corresponding relative-displacement response spectra) as a reference against which to check the accuracy of the long-period ground motions from a set of five accelerograph stations located within 5 km of the GPS stations. Conversely, we used the accelerograph data as a check on

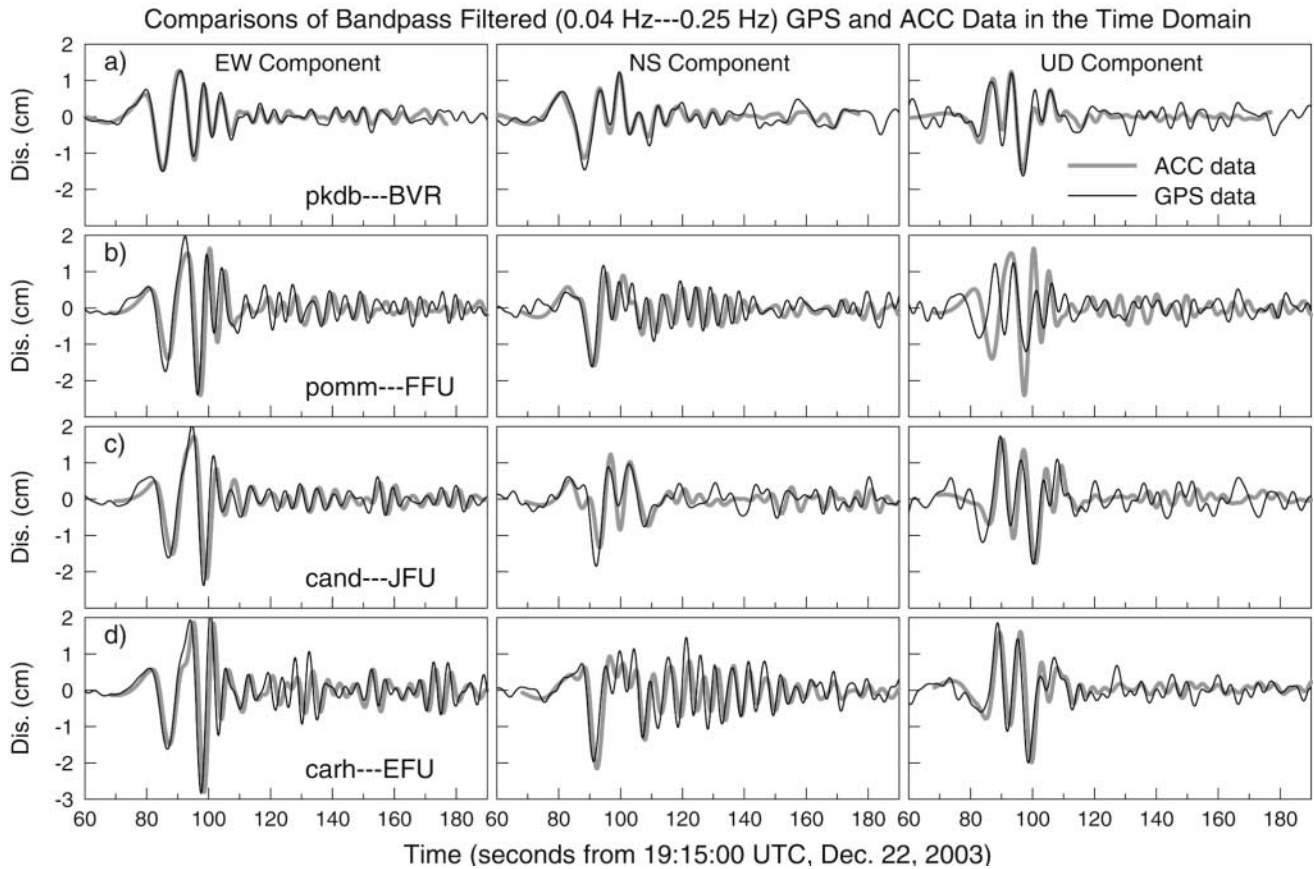


Figure 12. Comparisons of the bandpass-filtered accelerograph (ACC) and GPS data in the time domain (three components). The corner frequencies of the bandpass filter are set at 0.04 Hz and 0.25 Hz.

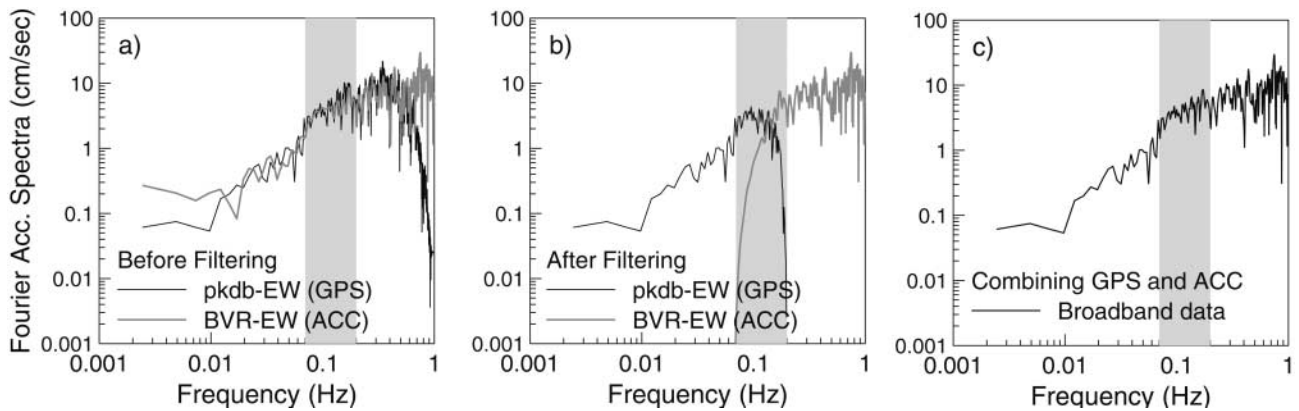


Figure 13. Plots illustrating the process of combining the accelerograph (ACC) (BVR-EW) and GPS (pkdb-EW) data in the frequency domain. The 1-sample-per-sec GPS data have been upsampled to 80 samples per sec by a cubic-spline interpolation before calculating the Fourier amplitude spectra. See text for details. The shaded regions indicate the transition band.

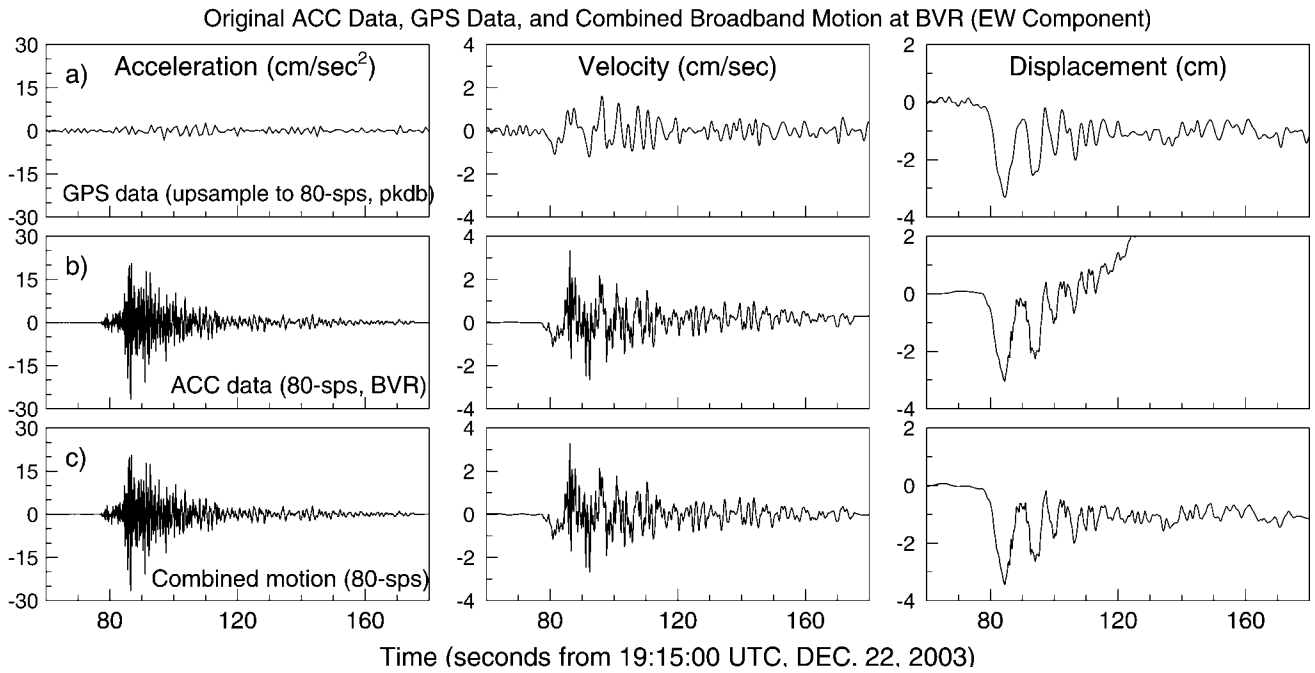


Figure 14. Comparisons of GPS data (pkdb-EW), accelerograph (ACC data (BVR-EW), and the broadband (BB) ground motion resulting from combining the GPS and ACC data. (a) Accelerations, velocities, and displacements from pkdb (GPS data, east-west component). (b) Accelerations, velocities, and displacements from BVR (original ACC data, east-west component). (c) Broadband ground motions from the combination of the collocated ACC and GPS data.

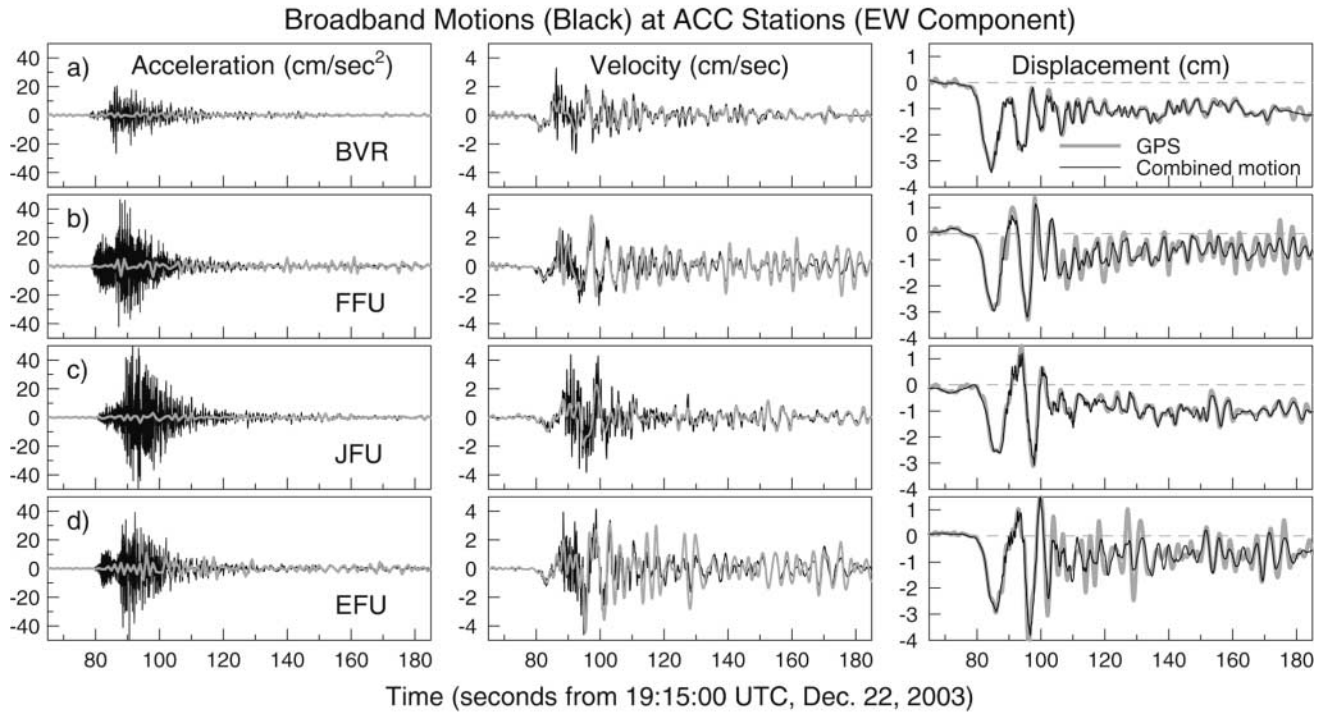


Figure 15. Broadband accelerations, velocities, and displacements at accelerograph (ACC) stations BVR, FFU, JFU, and EFU resulting from the combination of accelerograph recordings and collocated or closely spaced GPS recordings. GPS recordings at pkdb, pomm, cand, and carh are also plotted (gray) for comparison.

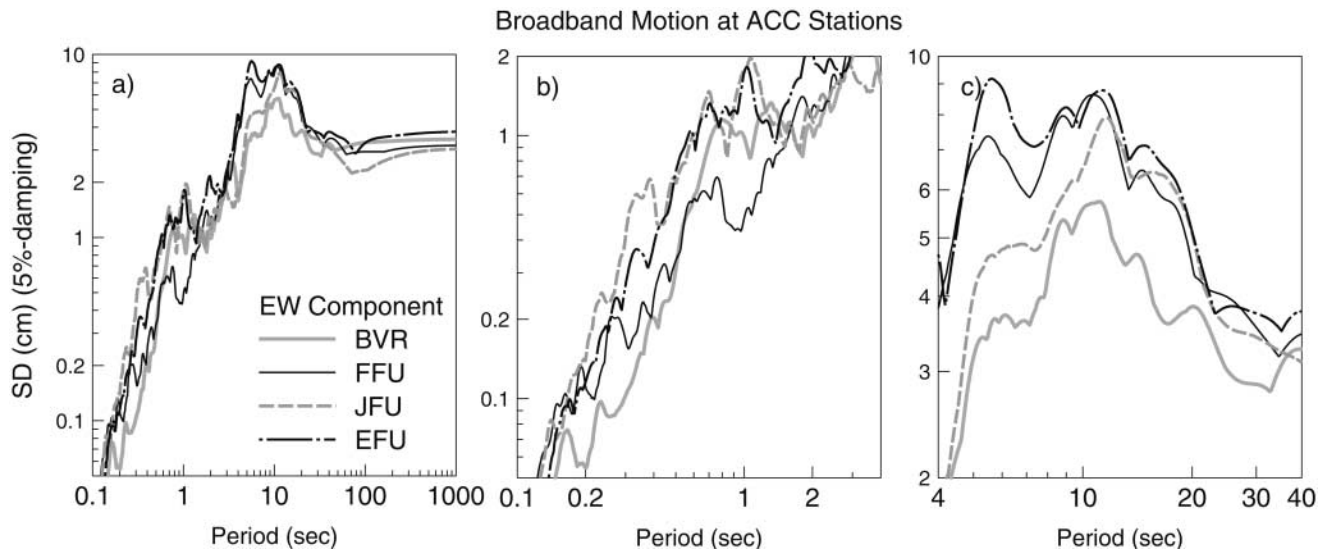


Figure 16. (a) 5%-damped relative-displacement response spectra (SD) calculated from the broadband motions obtained by combining the GPS and accelerograph (ACC) data. (b) and (c) are enlargements of the SD in two period ranges to show details. Note the different scales for the ordinates.

the high-frequency GPS motions. The GPS motions are clearly deficient in motions with periods less than 2 sec, as expected for data only sampled at 1 sample per sec. More importantly, the accelerographs provided good estimates of ground motions at periods up to and exceeding 30 sec. Significant spatial variability exists in the amplitudes of the ground motions, and in particular, the ground motions at GPS station pkdb (and the colocated Bear Valley Ranch accelerograph station) are lower than at the other Parkfield region stations. Similarly, the motions at the GPS station masw are higher than at other stations in the region. These differences extend over a wide range of frequencies, and it will be interesting to see if the differences persist for recordings of other earthquakes. We assume that the differences are due to variations in the geology in the region, but an explanation is beyond the scope of this article.

We combined the colocated or very closely spaced GPS and accelerograph data sets in the frequency domain to obtain a single broadband time series of the ground motion at each accelerograph station. These broadband ground motions may be useful to seismologists in unraveling the dynamic process of fault rupture and to engineers for designing large structures with very-long-period response.

### Acknowledgments

G.-Q. W. would like to thank Tom Herring for his patient guidance in operating his kinematic GPS data processing program "TRACK," Robert King for his kind help in installing GAMIT-GLOBK, and Yehuda Bock for many discussions regarding high-rate GPS data processing. Detailed reviews by John Langbein and Kristine Larson led to substantial improvements of the article. We benefited from several discussions with Chris Stephens. Finally, we would also like to acknowledge SOPAC (Script Orbit and Permanent Array Center) and CSRC (California Spatial Reference Cen-

ter) for making the GPS data freely available soon after the 2003 San Simon earthquake. This work was supported in part by NSF Grant GEO-0302967 and NASA Grant NNG15GN45G.

### References

- Bock, Y., L. Prawirodirdjo, and T. I. Melbourne (2004). Detection of arbitrarily large dynamic ground motions with a dense high-rate GPS network, *Geophys. Res. Lett.* **31**, L06604, doi 10.1029/2003GL019150.
- Bommer, J., and A. S. Elnashai (1999). Displacement spectra for seismic design, *J. Earthquake Eng.* **3**, 1–32.
- Boore, D. M. (2001). Effect of baseline correction on displacement and response spectra for several recordings of the 1999 Chi-Chi, Taiwan, earthquake, *Bull. Seism. Soc. Am.* **91**, 1199–1211.
- Boore, D. M. (2003). Analog-to-digital conversion as a source of drifts in displacements derived from digital recordings of ground acceleration, *Bull. Seism. Soc. Am.* **93**, 2017–2024.
- Boore, D. M. (2005a). Long-period ground motions from digital acceleration recordings: a new era in engineering seismology, in *Directions in Strong Motion Instrumentation*, P. Gülkan and J. G. Anderson (Editors), Springer, Dordrecht, The Netherlands, 41–54.
- Boore, D. M. (2005b). On pads and filters: processing strong-motion data, *Bull. Seism. Soc. Am.* **95**, 745–750.
- Boore, D. M., and J. Bommer (2005). Processing of strong-motion accelerograms: needs, options and consequences, *Soil Dyn. Earthquake Eng.* **25**, 93–115.
- Boore, D. M., J. F. Gibbs, W. B. Joyner, J. C. Tinsley, and D. J. Ponti (2003). Estimated ground motion from the 1994 Northridge, California, earthquake at the site of the interstate 10 and La Cienega Boulevard bridge collapse, west Los Angeles, California, *Bull. Seism. Soc. Am.* **93**, 2737–2751.
- Boore, D. M., C. D. Stephens, and W. B. Joyner (2002). Comments on baseline correction of digital strong-motion data: examples from the 1999 Hector Mine, California, earthquake, *Bull. Seism. Soc. Am.* **92**, 1543–1560.
- Borcherdt, R. D., J. B. Fletcher, E. G. Jensen, G. L. Maxwell, J. R. VanSchaack, R. E. Warrick, E. Cranswick, M.J.S. Johnston, and

- R. McClearn (1985). A general earthquake-observation system (GEOS), *Bull. Seism. Soc. Am.* **75**, 1783–1825.
- Brigham, E. O. (1988). *The Fast Fourier Transform and Its Applications*. Prentice Hall, Upper Saddle River, New Jersey, 448 pp.
- Chen, G. (1998). GPS kinematic positioning for the airborne laser altimetry at Long Valley, California, *Ph.D. Thesis*, Massachusetts Institute of Technology, available online at <http://geoweb.mit.edu/~tah/GChen> Thesis. (last accessed 10 August 2006)
- Choi, K., A. Bilich, K. M. Larson, and P. Axelrad (2004). Modified sidereal filtering: implications for high-rate GPS positioning, *Geophys. Res. Lett.* **31**, L22608, doi 10.1029/2004GL021621.
- Clinton, J. F. (2004). Modern digital seismology: instrumentation, and small amplitude studies in the engineering world, *Ph.D. Thesis*, California Institute of Technology, Pasadena, California.
- Converse, A. M., and A. G. Brady (1992). BAP—basic strong-motion accelerometer processing software, Version 1.0, *U.S. Geol. Surv. Open-File Rept. 92-296A*, 174 pp.
- Elósegui, P., J. L. Davis, D. Oberlander, R. Baena, and G. Ekström (2006). Accuracy of high-rate GPS for seismology, *Geophys. Res. Lett.* **33**, L11308, doi 10.1029/2006GL026065, 4 pp.
- Emore, G. L., J. S. Haase, K. Choi, K. M. Larson, and A. Yamagiwa (2007). Recovering absolute seismic displacements through combined use of 1 Hz GPS and strong motion accelerometers, *Bull. Seism. Soc. Am.* **97** (in press).
- Faccioli, E., R. Paolucci, and J. Rey (2004). Displacement spectra for long periods, *Earthquake Spectra* **20**, 347–376.
- Fletcher, J. B., L. M. Baker, P. Spudich, P. Goldstein, J. D. Sims, and M. Hellweg (1992). The USGS Parkfield, California, dense seismograph array: UPSAR, *Bull. Seism. Soc. Am.* **82**, 1041–1070.
- Genrich, J. F., and Y. Bock (1992). Rapid resolution of crustal motion at short ranges with the Global Position System, *J. Geophys. Res.* **97**, 3261–3269.
- Hanks, T. C. (1975). Strong ground motion of the San Fernando, California, earthquake; ground displacements, *Bull. Seism. Soc. Am.* **65**, 193–225.
- Harvey, D., and G. L. Choy (1982). Broadband deconvolution of GDSN data, *Geophys. J. R. Astr. Soc.* **69**, 659–668.
- Irwan, M., F. Kimata, K. Hirahara, T. Sagiya, and A. Yamagiwa (2004). Measuring ground deformations with 1-second sampled GPS data: the 2003 Tokachi-oki earthquake (preliminary report), *Earth Planets Space* **56**, 389–393.
- Iwan, W. D., M. A. Moser, and C.-Y. Peng (1985). Some observations on strong-motion earthquake measurement using a digital accelerograph, *Bull. Seism. Soc. Am.* **75**, 1225–1246.
- Ji, C., K. M. Larson, Y. Tan, K. W. Hudnut, and K. Choi (2004). Slip history of the 2003 San Simeon Earthquake constrained by combining 1-second sampled GPS, strong motion, and teleseismic data, *Geophys. Res. Lett.* **31**, L17608, doi 10.1029/2004GL020448.
- Langbein, J., and Y. Bock (2004). High-rate real-time GPS network at Parkfield: utility for detecting fault slip and seismic displacements, *Geophys. Res. Lett.* **31**, L15S20, doi 10.1029/2003GL019408.
- Larson, K. M., P. Bodin, and J. Gomberg (2003). Using 1-Hz GPS data to measure deformations caused by the Denali fault earthquake, *Science* **300**, no. 5624, 1421–1424.
- Miyazaki, S., K. M. Larson, K. Choi, and K. Hikima (2004). Modeling the rupture process of the 2003 September 25 Tokachi-Oki (Hokkaido) earthquake using 1-second sampled GPS data, *Geophys. Res. Lett.* **31**, L21603, doi 10.1029/2004GL021457.
- Nikolaidis, R. M., Y. Bock, P. J. de Jonge, P. Shearer, D. C. Agnew, and M. Van Domselaar (2001). Seismic wave observations with the Global Positioning System, *J. Geophys. Res.* **106**, 21,897–21,916.
- Wang, G.-Q., D. M. Boore, H. Igel, and X.-Y. Zhou (2003). Some observations on collocated and closely spaced strong ground-motion records of the 1999 Chi-Chi, Taiwan, earthquake, *Bull. Seism. Soc. Am.* **93**, 674–693.
- Wang, G.-Q., G. Tang, C. R. Jackson, X.-Y. Zhou, and Q. Lin (2006). Strong ground motions at the UPSAR during the 2003 San Simeon (M 6.5) and 2004 Parkfield (M 6.0) California, earthquakes, *Bull. Seism. Soc. Am.* **96**, S159–S182.
- Wdowinski, S., Y. Bock, J. Zhang, P. Fang, and J. Genrich (1997). Southern California permanent GPS geodetic array: spatial filtering of daily positions for estimating coseismic and postseismic displacements induced by the 1992 Landers earthquake, *J. Geophys. Res.* **102**, 18,057–18,070.
- Applied Geophysical Science Laboratories  
North Carolina A & T State University  
1020 E. Wendover Avenue  
Greensboro, North Carolina 27411  
wanggps@gmail.com  
gtang@ncat.edu  
(G.-Q.W., G.T.)
- U.S. Geological Survey, MS 977  
345 Middlefield Road  
Menlo Park, California 94025  
boore@usgs.gov  
(D.M.B.)
- College of Architectural and Civil Engineering  
Beijing University of Technology  
Beijing, 100022 China  
zhouxy@bjut.edu.cn  
(X.-Y.Z.)